organic compounds

High-Z′ and twinning behavior in 3,4-dinitrobenzoic acid

Matthias Zeller,[a]* Jake L. Stouffer,[a] Virgil C. Solomon[b] and Larry S. Curtin[a]*

[a]Department of Chemistry, Youngstown State University, One University Plaza, Youngstown, OH 44555, USA, and [b]Department of Mechanical and Industrial Engineering, Youngstown State University, One University Plaza, Youngstown, OH 44555, USA

Correspondence e-mail: mzeller@ysu.edu, lscurtin@ysu.edu

The title compound, $C_7H_4N_2O_6$, (I), crystallizes in $P\bar{1}$ with $Z' = 4$, but with no approximate or pseudosymmetry. The crystals were nonmerohedrally twinned, with at least four twin components related to the major moiety by 180° rotations around the real b and c axes, and by 180° rotation around the a^* axis. The excessive twinning is not caused by a phase change from an untwinned room-temperature higher-symmetry polymorph. The molecules are planar chiral and, owing to the tilt angle of the nitro groups and the position of protonation, there are altogether eight conformers possible. Six of these theoretically possible eight conformers are realized in the solid-state structure of (I). Packing analysis and force-field calculations indicate that the largest part of the packing interactions does not originate from the hydrogen-bonding interactions, as one might initially be tempted to assume; π–π stacking and $O_{nitro}\cdots\pi$ interactions between neighboring molecules of (I) seem to be the dominant factor that determines the packing observed in the structure of this nitro-substituted benzoic acid derivative.

Comment

Structures that crystallize with $Z' > 1$, *i.e.* structures that are built from more than one chemically identical but crystallographically distinct entity, have over the last decades become one of the focal points of crystallographic research. Around 8.8% of molecular solids crystallize with more than one crystallographically independent molecule per unit cell (Anderson *et al.*, 2006), but at this time the reasons for the phenomenon of crystallization are still not well understood. High-Z' structures are often associated with commensurate modulation, which can help to avoid mismatch of spacing between molecules in a simpler parent structure with a lower Z' value (Hao *et al.*, 2005). Pseudosymmetry or structure modulation is, however, not a necessary requirement for crystallization with $Z' > 1$, and most high-z' structures cannot

be reduced to a simpler parent structure with fewer crystallographically unique molecules. The two most cited reasons for the $Z' > 1$ phenomenon, for both modulated and non-modulated structures, are the non-self-complementary shape of the molecules, and competing strong directional interactions (Steed, 2003; Desiraju, 2007; Anderson & Steed, 2007; Anderson *et al.*, 2008). Specifically pointed out also was the formation of centrosymmetric synthons in combination with chirality of the molecules (Anderson *et al.*, 2006). As a consequence of these incompatibilities, there are many structures for which the observed $Z' > 1$ crystal does genuinely represent the most stable form, as the particular molecule simply cannot pack in a higher symmetry without generating highly unfavorable steric interactions, creating large lattice voids or sacrificing highly stabilizing directional interactions.

(I)
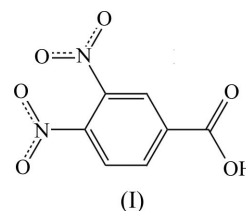
3,4-Dinitro-substituted benzoic acids are important precursors for the production of peripherally substituted metallotetraaza[14]annulenes (MTAAs). MTAAs are porphyrin analogs with either a planar or saddle-shaped geometry, depending on the substituents placed on the diiminato framework of the molecule (Weiss *et al.*, 1976, 1977; Ricciardi *et al.*, 1995; Mandon *et al.*, 1987; Wooodruff *et al.*, 1976). MTAAs have been extensively studied because when partially oxidized they become electronically conducting materials, while in their reduced forms they are electronic insulators. They can also be polymerized chemically or electrochemically *via* coupling at the diiminato proton (Ricciardi *et al.*, 1995; Bailey *et al.*, 1984, 1986*a*,*b*; Hochgesang & Bereman, 1988; Miry *et al.*, 2000). Electrochemically polymerized MTAAs are of particular value owing to the fact that their red/ox potentials can be tuned depending on the electron-donating or -withdrawing characteristics of the peripheral substituents. In addition to their unique electrochemical properties, they also have interesting optical properties, being black in the oxidized form and golden in their reduced form. During our investigations into the synthesis and properties of MTAAs, we attempted to synthesize several derivatives of (I) as starting materials for the synthesis of MTAAs. As the structure of the parent 3,4-dinitrobenzoic acid was as yet unknown, we attempted to establish its single-crystal structure for comparison and reference purposes. The structures of 2,4-dinitrobenzoic acid [Cambridge Structural Database (CSD) refcode BIPJUF; Wieckowski & Krygowski, 1985] and 2,5-dinitrobenzoic acid (DAJXUH; Grabowski & Krygowski, 1985) had been reported in the 1980s, and two polymorphs of 3,5-dinitrobenzoic acid [CUKCAM01 in $P2_1/c$ (Prince *et al.*, 1991) and CUKCAM02 in $C2/c$ (Kanters *et al.*, 1991; Domenicano *et al.*, 1990)] have been described. The structure of 3,4-dinitrobenzoic acid was, however, suspiciously unknown.
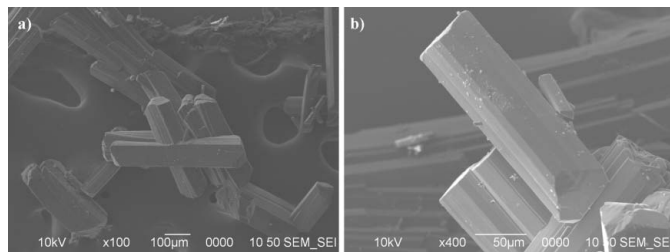
organic compounds

Figure 1
SEM micrographs of crystals of 3,4-dinitrobenzoic acid. (*a*) A selection of crystals typical of the batch as a whole at 100× magnification. (*b*) A not intergrown crystal at 400× magnification showing the layering of twin domains (lighter and darker areas within apparently single crystals). Crystals were gold–palladium coated for SEM imaging.

Initial attempts to grow single crystals of (I) and collect data were hampered by a tendency of the compound to form excessively twinned crystals. Crystals of (I) were grown from a variety of solvents, including water, ethanol–water and deuterated chloroform (see *Experimental*). Crystals did readily form from any of these solvents and all crystallization attempts yielded the same solvent-free polymorph, but specimens from all batches suffered from excessive nonmerohedral twinning. Prompted by the excessive twinning, the samples were also analyzed by scanning electron microscopy (SEM) analysis. A representative selection of crystals was mounted on carbon tape and Pd–Au coated for SEM analysis. Crystals imaged by SEM were typically rod shaped, with lengths of up to *ca* 0.4 mm, and on average slightly less than 100 µm wide, but much smaller crystals were also present. Most crystals were intergrown and clearly not single, with crystals aligned at various angles between 60 and 80°, leading to intersecting rods as shown in Fig. 1(*a*), or at angles less than 10°, thus forming frayed rods with an irregular shape instead of clear crystal faces. Some crystals, such as the specimen shown in Fig. 1(*b*), appeared well formed, with clearly defined crystal faces. Even these well formed crystals, however, showed clear signs of twinning in the form of layers that stretch throughout the crystals along the long axis of the rods (dark and light gray layers in Fig. 1*b*). The thickness of the twin domains varies between just a few and up to a few dozen micrometres. At the resolution of the SEM images, the layered twin domains formed this way are perfectly parallel with one another, thus not affecting the shape or macroscopic appearance of the crystallites. The SEM images thus revealed that all specimens selected were macroscopically twinned, but even the largest twin domains were only a few dozen micrometres thick, thus making it impossible to isolate an untwinned sample still large enough to use for single-crystal X-ray diffraction with a normal laboratory sealed-tube X-ray source. Based on the SEM micrograph observations, we thus screened multiple crystals from all batches for both diffraction intensity and degree of twinning (see *Refinement* for details). The least twinned specimens had still at least four major twin components which originated from the major moiety by 180° rotations around the real *b* and *c* axes, and by a 180° rotation around the *a** axis. In all samples for which partial data were
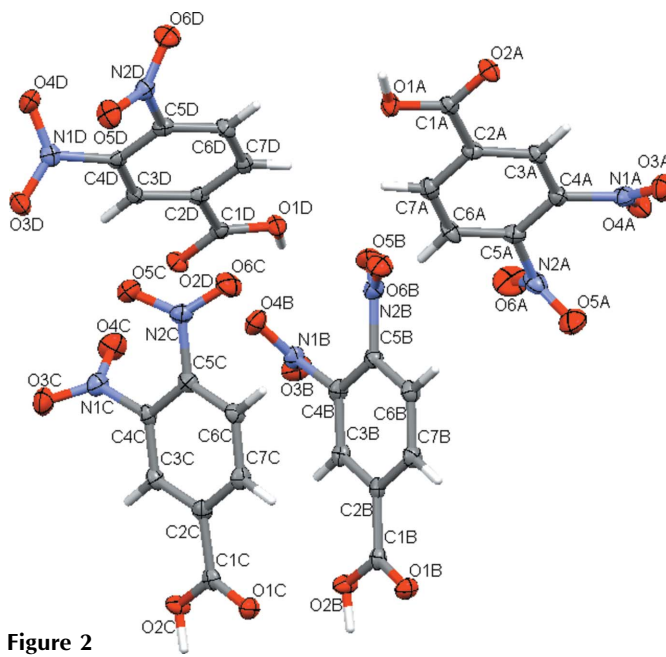

Figure 2
Plot of the crystallographically independent section of the structure of 3,4-dinitrobenzoic acid. Displacement ellipsoids of non-H atoms are drawn at the 50% probability level. H atoms are represented as capped sticks.

collected, the data overlap of neighboring spots was substantial, with many spots showing multiple consecutive overlaps in a 'chain-of-pearls' fashion, and many diffraction spots were thus automatically rejected by the integration program (*SAINT*; Bruker, 2009). For a recent example of a twinned structure suffering from similar excessive consecutive peak overlay problems, see Kumar *et al.* (2010). The crystal of (I) eventually selected for a complete data collection (a fragment of a larger crystal) showed a rejection rate of around 30–40%, and collection of a full sphere of data *via* ω scans led to a 96% complete data set up to 25° (with molybdenum radiation). Additional collection of φ scans did not significantly increase the completeness of the data set any further. The distribution of the data among the four twin domains is shown in Table S1 in the *Supplementary materials*, and the exact twin matrices identified by the integration program are given in supplementary Table S2.

The title compound crystallizes in the space group $P\bar{1}$ with four crystallographically independent molecules per unit cell. A displacement ellipsoid plot of the symmetry-independent molecules *A* through *D* is shown in Fig. 2. The configurations of the four independent molecules in the lattice show substantial variation. There are four independent variables that formally define the molecular geometry of the 3,4-dinitrobenzoic acid molecules upon crystallization and freezing out of fast equilibration through either proton transfer or rotation of the nitro groups. The 3,4-dinitro substitution makes the molecules planar chiral. The place of protonation at the carboxylic acid group in relation to the position of the nitro groups transforms the two planar chiral enantiomers into two diastereomeric pairs of enantiomers. The nitro groups in the molecules of (I) are, however, not
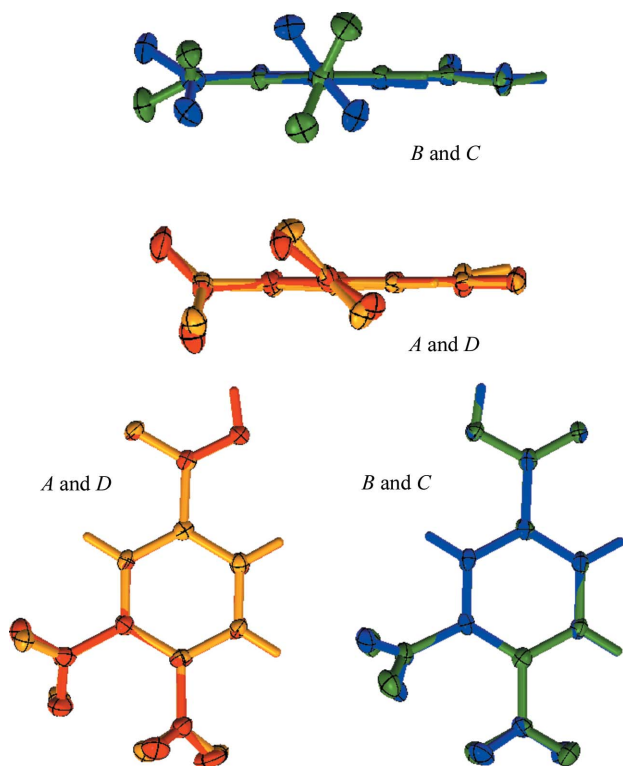
Figure 3
Least-squares overlay of molecules *A* and *D* (red and orange in the electronic version of the paper) and *B* and *C* (blue and green in the electronic version of the paper) in top and side view. Molecules *A* and *D* have identical conformations with both the position of protonation as well as the tilt direction of the nitro groups being the same. In molecules *B* and *C*, the site of protonation is switched when compared to *A* and *D*. *B* and *C* are not superimposable with each other and are differentiated by the tilt direction of the nitro groups.

Figure 4
Packing view of the structure of 3,4-dinitrobenzoic acid, viewed down the *a* axis. The color coding is as in Fig. 3.

coplanar with the plane of the benzene ring, thus adding two more variables that define the molecular geometry of the molecules. Common to all four molecules observed in the solid-state structure are the approximate absolute values of the angles between the benzene and nitro groups, which vary between 26.4 (2) and 64.8 (2)°. Also common to all molecules is that the direction of rotation of the two nitro groups within each molecule is necessarily linked, *i.e.* the nitro groups in each molecule are tilted in the same direction in order to avoid close $O_{nitro} \cdots O_{nitro}$ contacts between neighboring substituents. The tilt direction of the NO_2 groups can thus be handled as one single variable for each molecule. Adding this variable to the inherent planar chiral nature of the molecule and the position of protonation creates eight possible non-superimposable stereoisomers for the molecules of (I), or four diastereomeric pairs of enantiomers. Of the possible four types of diastereomers, three are realized in the solid-state structure of (I). Taking the centrosymmetry of the structure into account, six of the theoretically possible eight enantiomers are observed. Fig. 3 shows how the molecules are related. A least-squares overlay of molecules *A* and *D* shows them to have identical conformations, with both the position of protonation as well as the tilt direction of the nitro groups being the same with respect to the position of the nitro
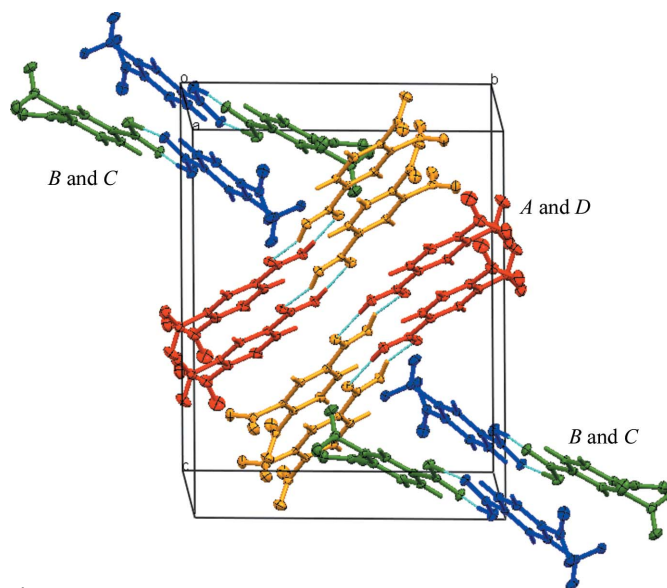
substituents. In molecules *B* and *C*, the site of protonation is switched when compared to *A* and *D*. In *B* and *C*, the hydroxy group is located on the same side as the nitro group, while in *A* and *D* it is on opposite sides. *B* and *C* are, in contrast to *A* and *D*, not superimposable with each other and form members of two different groups of diastereomers differentiated by the tilt direction of the nitro groups (Fig. 3).

The tilt angles of the nitro groups against the planes of the benzene rings are mostly within the ranges seen in other aromatic nitro compounds. Only for molecule *C* is one of the dihedral angles significantly larger than one would expect [64.8 (2)°, plane of C2*C*–C7*C*/N1*C* against C4*C*/N1*C*/O3*C*/O4*C*], and a comparison with other similar molecules flagged this torsion angle as unusually large. Out of 10 000 entries in the CSD, only 618 had nitro–benzene torsion angles of 65° or higher. It should be noted that molecule *C* also has the smallest of all nitro–benzene torsion angles, *viz.* 26.4 (2)° for the nitro group of N2*C*, and steric interaction of this nitro group, which is nearly coplanar with the aromatic ring, is a possible reason for the unusually large nitro–benzene torsion angle of 64.8 (2)° for the nitro group of N1*C*. All other molecular parameters of all four molecules are within the expected ranges for this type of molecule [CSD *Mogul* geometry check (Macrae *et al.*, 2008; CCDC, 2009), based on CSD Version 5.32, November 2010 (Bruno *et al.*, 2002)].

The molecules are arranged as dimers connected *via* pairwise hydrogen bonds, with the motif typical for carboxylic acids [graph-set motif $R_2^2(8)$; Bernstein *et al.*, 1995] (Table 1). Molecules *A* form pairs with molecules *D*, and molecules *B* form pairs with molecules *C* (Fig. 4). Both dimers are pseudocentrosymmetric, with the nitro groups in the 3- and 4-positions of the two benzene rings related by noncrystallographic inversion centers located in the center of the hydrogen-bonded carboxylic acids, but none of the dimers are actually centrosymmetric in the solid state (no crystal-
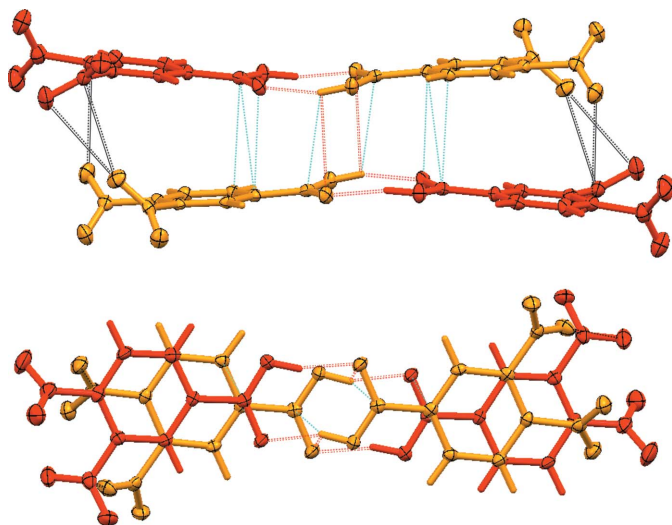
Figure 5
Pairs of dimers of molecules *A* and *D* (color coding as in Fig. 3). Double dotted lines (red in the electronic version of the paper) are O—H···O hydrogen bonds (including the weak H1*D*···O2*D* interaction), single dotted lines (blue) are significant π–π stacking interactions, and mixed solid/dotted lines (black) are O_{nitro}···π interactions.

lographic inversion centers relate the two molecules of the dimers with each other).

Both the *AD* and *BC* dimers are arranged in double layers of parallel dimers with a substantial π–π stacking interaction component. The perpendicular distances between the average molecular planes of the dimers, as defined by all non-H atoms, apart from the nitro O atoms of each dimer, are 3.447 Å for the plane of the *AD* dimers and 3.349 Å for that of the *BC* dimers.

Individual pairs of dimers are, however, slightly offset, as shown in Fig. 5 for the pair of *AD* dimers. The dimers are closest towards the center of the pair of dimers, with a distance between planes of less than 3 Å (the H1*D*···O2*D* distance is 2.94 Å, indicating the possibility of the hydrogen bond from O1*D*—H1*D* being bifurcated and having, in addition to the main hydrogen bond towards O2*A*, a smaller component towards O1*D*). Towards the tail ends of the pair of dimers, the planes move further apart, probably due to the tilting of the nitro groups of molecule *D*, which exhibit through their O atoms close contacts with the π-electron density of the nitro and benzene groups of molecule *A*. Fig. 5 shows a summary of these interactions: O—H···O hydrogen bonds (including the possible weak H1*D*···O2*D* interaction), significant π–π stacking interactions at the center of the pairs of dimers, and the most important O_{nitro}···π interactions towards the fringe of the double dimeric assemblies.

The *BC* pairs of dimers are arranged in a slightly different way (Fig. 6). The center of symmetry that connects the two dimers is, as in the case of *AD*, shifted, not along the direction of the axis of the dimers, but perpendicular to this axis. The *BC* dimers thus are shifted sideways against each other and mostly do not come to rest atop of one another. As a consequence, the number of direct contacts involving the π–π stacking interactions is much lower for the *BC* pairs of dimers than for
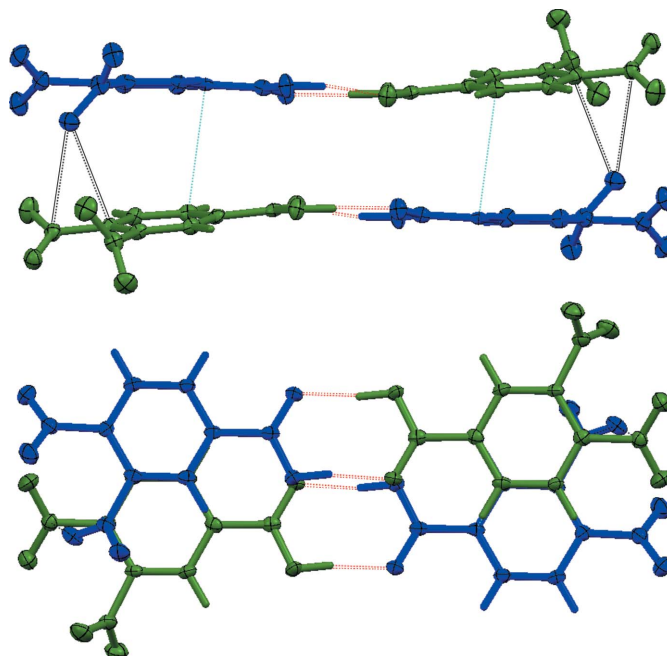

Figure 6
Pairs of dimers of molecules *B* and *C* (color coding as in Fig. 3). Double dotted lines (red in the electronic version of the paper) are O—H···O hydrogen bonds, single dotted lines (blue) are significant π–π stacking interactions, and mixed solid/dotted lines (black) are O_{nitro}···π interactions.

AD, and no additional hydrogen-bonding interactions between the dimers are possible. O_{nitro}···π interactions are limited to that between one nitro O atom of molecule *B* and one nitro π-system of molecule *C*.

The pairs of dimers, both *AD* and *BC*, are translated along the *a* axis of the cell, leading to infinite double strands of π-stacked parallel molecules. Perpendicular to the *a* axis, the infinite *AD* and *BC* strands are tilted against each other and are arranged in a herringbone fashion (Fig. 7). The tilt angle of the planes, again defined by all non-H atoms, with the exception of the nitro O atoms of each *AD* and *BC* dimer, is 65.69°.

Using UNI force-field calculations, approximate energies for intermolecular potentials were estimated (Gavezzotti, 1994; Gavezzotti & Filippini, 1994), yielding a total packing energy of −527.0 kJ mol^{-1}. Intermolecular potentials given are the sum of Coulombic, polarization, dispersion and repulsion terms, as defined in the PIXEL method. Hydrogen-atom positions were normalized prior to the calculations, *viz.* O—H distances to 0.993 Å and C—H distances to 1.089 Å. Among the significant interactions found were, of course, the intermolecular potentials associated with the two $R_2^2(8)$ hydrogen-bonding interactions, with values of −40.9 and −32.3 kJ mol^{-1} for the *CB* and the *AD* dimers, respectively. These interactions were, however, not the strongest interactions, but were ranked by the force-field calculation only as fourth and sixth. Altogether, six substantial interactions with a stabilization energy of over 30 kJ mol^{-1} were detected, with four of them, including the strongest ones, being stacking interactions between the molecules of (I). The largest inter-
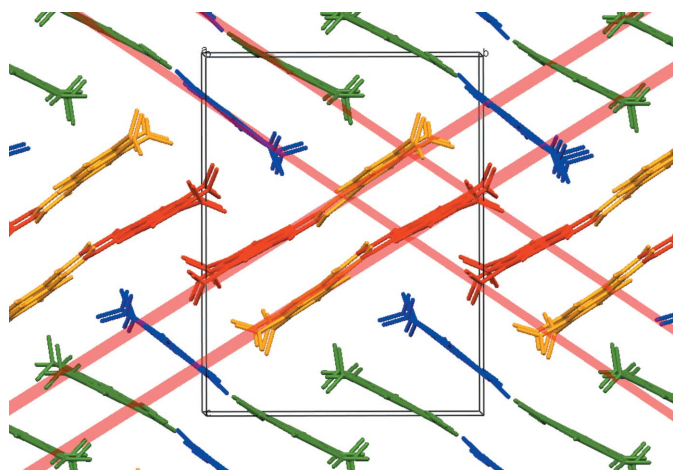
Figure 7
Depiction of the infinite double strands of π-stacked parallel molecules, viewed down the *a* axis. Perpendicular to the *a* axis, the infinite *AD* and *BC* strands are tilted against each other and arranged in a herringbone fashion with a tilt angle of the planes (indicated in opaque red in the electronic version of the paper) of 66.15°.

molecular potential, at -45.6 kJ mol^{-1}, is observed between two of the *C* molecules across a crystallographic inversion center. The second strongest, at -44.4 kJ mol^{-1} nearly as pronounced, is a stacking interaction between molecules *A* and *D*. In this case, the molecules are parallel to one another, and not related by inversion symmetry. Interestingly, all strong interactions above 30 kJ mol^{-1} are between either the *A* and *D*, or between the *B* and *C* molecules. No such interactions are found between *A* and *B* or *C*, or *D* and *B* or *C*, thus indicating the formation of two separate 'regions' or 'clusters' within the structure, with no strong interactions between molecules of the two regions. The force-field calculations thus agree with and substantiate the results of the sum of the individual interactions as discussed in the packing arrangements section above, but indicate that the largest part of the packing interactions does not originate from the hydrogen-bonding interactions, as one might initially be tempted to assume; indeed, the π–π stacking and O$_{nitro}$···π interactions between neighboring molecules of 3,4-dinitrobenzoic acid molecules are the dominant factor that determines the packing observed in the structure of this nitro-substituted benzoic acid.

Equivalent calculations were performed for the 2,4- and 2,5- and the two 3,5-isomers of dinitrobenzoic acid [BIPJUF and DAJXUH (Wieckowski & Krygowski, 1985; Grabowski & Krygowski, 1985); CUKCAM01 in *P*2$_1$/*c* (Prince *et al.*, 1991), and CUKCAM02 in *C*2/*c* (Kanters *et al.*, 1991; Domenicano *et al.*, 1990)]. The two polymorphs of the 3,5-isomer are structurally related, and the conformations of the molecules and their arrangement in hydrogen-bonded dimers in the two structures are virtually identical. The packing of the dimeric units is also related, with layers two molecules thick along the *a* axes of both structures being superimposable. The structures are distinguished by the nature of the successive layers along this axis: in the primitive *P*2$_1$/*c* structure, the third and fourth layers are located in the next unit cell and are created by

translation; in CUKCAM02, the third and fourth layers are part of the larger *C*-centered cell and a result of the twofold axis being present only in this double-volume cell but not in the primitive setting of CUKCAM01 (overlays and comparisons of CUKCAM01 and CUKCAM02 are provided as supplementary figures S1 and S2 in the *Supplementary materials*).

The force-field calculations performed for the 2,4- and 2,5- and the two 3,5-isomers of dinitrobenzoic acid do not mirror the results for 3,4-dinitrobenzoic acid. In all of these four structures, the $R_2^2(8)$ hydrogen-bonding interactions were significantly more pronounced than in 3,4-dinitrobenzoic acid, with individual intermolecular potentials between -46.59 and -48.61 kJ mol^{-1} (for the *P*2$_1$/*c* polymorph of the 3,5-isomer and the 2,4-isomer, respectively). Only for the 2,5-isomer was the intermolecular potential associated with the $R_2^2(8)$ hydrogen bond not the strongest individual interaction. In this molecule, an intermolecular interaction associated with a strong symmetric π-stacking interaction, with an interplanar separation of 3.54 Å, was attributed -49.32 kJ mol^{-1}, *versus* -47.74 kJ mol^{-1} for the potential associated with the $R_2^2(8)$ hydrogen bond. These results point towards a substantial weakening of the hydrogen-bonding interactions in 3,4-dinitrobenzoic acid when compared to its 2,4- and 2,5- and the two 3,5-isomers, with stabilization energies for the two hydrogen bonds in the 3,4-isomer that are around 7 and 15 kJ mol^{-1} weaker than their counterparts in the 2,4- and 2,5- and the two 3,5-isomers. Compared to other aromatic carboxylic acid dimers, the weakening of the hydrogen bonds in 3,4-dinitrobenzoic acid seems to be even more pronounced. Values reported by Gavezotti using the same method (PIXELS) were generally lower than -50 kJ mol^{-1} and clustered around -70 kJ mol^{-1} (Gavezzotti, 2008).

An analysis of the actual hydrogen-bonding parameters in the structure of (I) does provide some additional evidence for a diminished hydrogen-bonding strength. The O···O distances within all five structures are, after correction for the different data-collection temperatures (the current data set was collected at 100 K, all others were collected at room temperature), comparable with each other, but those of the 3,4-isomer appear to be somewhat elongated when compared to those of the other isomers. The values for the 2,4- and 2,5- and the two 3,5-isomers at room temperature are 2.656, 2.622, 2.633 and 2.636 Å, respectively; those for the 3,4-isomer at 100 K are 2.607 (4) and 2.619 (4) Å for the *AD* dimer, and 2.604 (4) and 2.615 (4) Å for the *BC* dimer. Correction of these values for the difference in data-collection temperature, *e.g.* by 0.048 Å, as was observed for 2,4,6-trimethylbenzoic acid (CSD entries TMBZAC02 to TMBZAC05; Wilson & Goeta, 2004), would raise the O···O distances above those observed for the other isomers by 0.021 and 0.025 Å for the *BC* and the *AD* dimers, respectively. While these values might be able to explain some of the weakening of the hydrogen bonds, they seem not substantial enough to explain the full 7 and 15 kJ mol^{-1} loss in stabilization predicted by the UNI force-field calculations. The total packing energies per molecule indicated a slightly more favorable packing arrangement

organic compounds

for the 2,4- and 2,5- and the two 3,5-dinitrobenzoic acids when compared to the 3,4-isomer (−132.88, −135.13, −132.11 and −133.37 kJ mol^{-1} *versus* −131.75 kJ mol^{-1} per molecule, respectively).

In their 2006 paper on the prevalence of large Z' values in systems that can form tightly hydrogen-bonded dimeric structures, Steed and co-workers (Anderson *et al.*, 2006) analyzed carboxylic acid derivatives and similar molecules for their tendency to form high-Z' structures. For carboxylic acid derivatives such as the title compound, they found that there is indeed a connection between the ability of a system to form an $R_2^2(8)$ COOH dimer motif and the number of crystallographically independent molecules in the structure, but that this Z' behavior is limited to only chiral carboxylic acid structures. If they crystallize in a nonchiral setting they do not behave significantly differently from other organic compounds as a whole [chiral structures containing the COOH dimer motif crystallize with $Z' > 1$ in 13.9% of cases, compared with 10.7% for achiral carboxylic acids and 8.8% of structures in the CSD as a whole (Anderson *et al.*, 2006)].

High Z' values are often associated with pseudosymmetry, and pairs of molecules tend to be related to each other by approximate translations, rotations or centers of symmetry. Many of these structures only deviate slightly from higher symmetry, with only small energetic differences between the high-Z' form and a (hypothetical) higher-symmetry form. As a consequence, higher-temperature polymorphs can often be found in which the differences between crystallographically independent molecules present in the low-temperature polymorph are lost. Often associated with a phase change from a higher-symmetry high-temperature form to the lower-symmetry low-temperature form is twinning (pseudo-merohedral and/or nonmerohedral). As the crystals of the title compound are heavily twinned by several nonmerohedral twin operations, the structure was thus investigated for the possible presence of pseudosymmetry or temperature-dependent phase changes. A *PLATON* analysis for missed symmetry did not however yield any additional pseudosymmetry or pseudo-translation, even with the most relaxed search criteria (Spek, 2009). This is in agreement with the already described presence of six of the theoretically possible eight enantiomers in the crystal structure (see molecular geometry discussion). The presence of so many conformationally different molecules makes an arrangement of similar entities related by pseudo-symmetry and especially pseudo-translation difficult to realize.

To more confidently rule out any pseudosymmetry as the cause for either the high Z' value or the pronounced twinning, the crystals were tested for the possible presence of a phase change between room temperature and 100 K. The unit cells found at room temperature differed only marginally from those at 100 K, and no difference with regard to the degree or type of twinning was observed. The presence of twinning at room temperature, and not only upon cooling to 100 K, is also confirmed by the room-temperature SEM images (Fig. 1), which revealed clear signs of excessive twinning for all crystals analyzed. The structure of (I) described here thus seems to be a genuine $Z' = 4$ structure with no approximate or pseudo-

symmetry, and the excessive twinning observed is not caused by a phase change from an untwinned room-temperature higher-symmetry polymorph. This is also supported by the fact that crystals of (I) grown by three different methods from different solvents yielded the same polymorph and all crystals from all batches showed the same types of twinning, regardless of the way they had been grown (slow cooling of a hot aqueous solution, slow evaporation of a chloroform solution, or vapor diffusion of water into an ethanol solution at constant temperature). This points towards the observed polymorph of (I) with $Z' = 4$ to be the actual thermodynamically most stable crystal form (but this cannot be ascertained with absolute surety, of course), which raises the question of what causes the molecule to crystallize in this complicated high-Z' structure. The reasons for compounds to crystallize with more than one crystallographically independent molecule are manifold, and no single principle can be found to explain the $Z' > 1$ phenomenon. However, some causes seem to be observed on a regular basis that are associated with a higher than usual tendency to crystallize with $Z' > 1$: a non-self-complementary shape of the molecules, and competing strong directional interactions (Steed, 2003; Desiraju, 2007; Anderson & Steed, 2007; Anderson *et al.*, 2008). For 3,4-dinitrobenzoic acid, both of these causes seem to play a role, but in particular competition between strong directional hydrogen-bonding interactions and other less directional (but in their sum equally strong forces, such as π–π stacking and $O_{nitro}\cdots\pi$) interactions seem to affect the molecules' ability to pack in a simple regular arrangement. The packing with a high Z' value is made easier by the number of possible conformations that the molecule can assume. By realizing six of the eight energetically comparable conformers in the solid state, 3,4-dinitrobenzoic acid is able to achieve a solid-state arrangement in which competition between hydrogen-bonding, π–π stacking and $O_{nitro}\cdots\pi$ interactions is balanced to a degree to allow for effective packing, with a total packing energy similar to that observed for the other isomers of dinitrobenzoic acid that do not suffer as much from packing frustration as the 3,4-isomer.

Experimental

3,4-Dinitrobenzoic acid (99%) was obtained from Alfa–Aesar. Crystallization was first accomplished by serendipitous crystal formation from deuterated chloroform in an NMR tube. Crystals from this batch, and from other attempts using chloroform as the solvent, yielded only excessively twinned samples not suitable for X-ray diffraction (see *Refinement* for details regarding the twinning). Slow diffusion of water into a solution of (I) in ethanol yielded well formed crystals, but the crystals were still excessively twinned and none of several set-ups with different solvent and compound ratios yielded crystals suitable for X-ray single-crystal diffraction. In another attempt to obtain X-ray-quality crystals, deionized water was used, and crystallization was achieved by heating small samples of saturated solutions to boiling followed by slow cooling, or by slow cooling of room-temperature solutions to 277.5 K. The crystals obtained that way were somewhat improved, with fewer twin domains and diffraction spot overlaps, but still not suitable for

collection of a usable X-ray data set. An increase of both solvent volume and sample amount (using a 100 ml Erlenmeyer flask and several grams of 3,4-dinitrobenzoic acid), to achieve a decreased cooling rate and slower crystal growth (and thus larger domain sizes and less twinning), still led to crystals that were mostly excessively twinned. Among the bulk of these samples, some crystals were however identified as possible candidates for data collection, and these specimens were chosen for crystal screening (see *Refinement*).

Crystal data

$C_7H_4N_2O_6$	$\gamma = 84.838\ (11)°$
$M_r = 212.12$	$V = 1610\ (2)$ Å^3
Triclinic, $P\bar{1}$	$Z = 8$
$a = 7.373\ (6)$ Å	Mo $K\alpha$ radiation
$b = 13.06\ (1)$ Å	$\mu = 0.16$ mm^{-1}
$c = 16.800\ (12)$ Å	$T = 100$ K
$\alpha = 89.633\ (12)°$	$0.25 \times 0.09 \times 0.06$ mm
$\beta = 88.194\ (12)°$	

Data collection

Bruker SMART APEX CCD diffractometer	34980 measured reflections
Absorption correction: multi-scan (*TWINABS*; Bruker, 2008)	7991 independent reflections
$T_{min} = 0.935$, $T_{max} = 1.000$	6572 reflections with $I > 2\sigma(I)$
	$R_{int} = 0.088$

Refinement

$R[F^2 > 2\sigma(F^2)] = 0.062$	H atoms treated by a mixture of restrained and constrained refinement
$wR(F^2) = 0.164$	
$S = 1.07$	
7991 reflections	$\Delta\rho_{max} = 0.33$ e Å^{-3}
552 parameters	$\Delta\rho_{min} = -0.39$ e Å^{-3}
6 restraints	

The crystals of the sample were found to be excessively non-merohedrally twinned. SEM imaging of several representative crystals indicated the presence of macroscopic twin domains, but individual domains were not larger than just a few micrometres, and on average much smaller (see Fig. 1*b*). Multiple crystals were screened and orientation matrices for the twin components were identified using the program *CELL_NOW* (Bruker, 2005). From the tested crystals about half a dozen were selected for partial data collection based on their diffraction power, the number of twin components present, and the degree of overlap of the twin components. All of these final crystals had at least four major twin components created from the major component by 180° rotations around the real axes [010] and [001], and by 180° rotation around the reciprocal axis (100). In all samples for which partial data were collected, the data overlap of neighboring spots was significant, with many spots showing multiple consecutive overlaps in a 'chain of pearls' fashion, and many diffraction spots were thus automatically rejected by the integration program (*SAINT*; Bruker, 2009). Most integrated data showed rejection rates of 50% and above. Attempts to collect data at a larger crystal-to-detector distance did not significantly lower the number of rejected reflections. The crystal selected for a complete data collection (a fragment of a larger crystal) showed a rejection rate of around 30–40%. Data were collected with 90 s exposure time per frame at 100 K. Collection of a hemisphere of data using ω scans yielded a data set slightly less than 80% complete. Collection of the other half of the full sphere led to a 93% complete data set up to 26.37° in θ, and 96% to 25°. Additional collection of φ scans did not significantly increase the completeness of the data set any further.

Table 1
Hydrogen-bond geometry (Å, °).

D—H$\cdots A$	D—H	H$\cdots A$	$D\cdots A$	D—H$\cdots A$
O1A—H1$A\cdots$O2D^{i}	0.93	1.71	2.619 (4)	163
O2B—H2$B\cdots$O1C^{ii}	0.93	1.70	2.615 (4)	169
O2C—H2$C\cdots$O1B^{ii}	0.93	1.68	2.604 (4)	172
O1D—H1$D\cdots$O2A^{iii}	0.92	1.75	2.607 (4)	154

Symmetry codes: (i) $x - 1, y, z$; (ii) $-x + 2, -y, -z$; (iii) $x + 1, y, z$.

The twin laws found by *CELL_NOW* for the final crystal chosen were a rotation from the first domain by 180° about reciprocal axis (010) (domain 2), a 180° rotation about reciprocal axis (001) (domain 3), and a 180° rotation about the real axis [100] (domain 4).

The distribution of the data among the four twin domains is shown in Table S1, and the exact twin matrices identified by the integration program in Table S2 in the *Supplementary materials*.

The final data were corrected for absorption using *TWINABS* (Bruker, 2008), and the structure was solved using direct methods with only the non-overlapping reflections of component 1. Using the HKLF5 least-square refinement method for nonmerohedrally twinned crystals as specified in *SHELXL* (Sheldrick, 2008), the structure was refined with all reflections of component 1 (including all overlapping diffraction spots) with a resolution better than 0.8 Å, resulting in BASF values of 0.071 (1), 0.191 (1) and 0.061 (1).

The total number of reflections given (`_diffrn_reflns_av_R_equivalents`) is before the cutoff at 0.8 Å. The R_{int} value given is for these reflections and is based on agreement between observed single and composite intensities and those calculated from refined unique intensities and twin fractions before the cutoff at 0.8 Å.

H atoms attached to C atoms were positioned geometrically and constrained to ride on their parent atoms, with C—H distances of 0.95 Å, and with U_{iso}(H) = $1.2U_{eq}$(C). The hydroxy H atoms were refined in calculated positions at a fixed C—O—H angle, but the C—C—O—H dihedral angle and the O—H distance were allowed to refine (AFIX 148 command in *SHELXTL*; Sheldrick, 2008), and with U_{iso}(H) = $1.5U_{eq}$(O). The O—H distances in the four crystallographically independent molecules were restrained to be the same within a standard deviation of 0.02 Å.

Data collection: *APEX2* (Bruker, 2009); cell refinement: *SAINT* (Bruker, 2009); data reduction: *SAINT* and *TWINABS* (Bruker, 2008); program(s) used to solve structure: *SHELXTL* (Sheldrick, 2008); program(s) used to refine structure: *SHELXTL*; molecular graphics: *SHELXTL*; software used to prepare material for publication: *SHELXTL* and *publCIF* (Westrip, 2010).

References

Anderson, K. M., Afarinkia, K., Yu, H.-W., Goeta, A. E. & Steed, J. W. (2006). *Cryst. Growth Des.* **6**, 2109–2113.
Anderson, K. M., Goeta, A. E. & Steed, J. W. (2008). *Cryst. Growth Des.* **8**, 2517–2524.
Anderson, K. M. & Steed, J. W. (2007). *CrystEngComm*, **9**, 328–330.
Bailey, C. L., Bereman, R. D., Rillema, D. P. & Nowak, R. (1984). *Inorg. Chem.* **23**, 3956–3960.

organic compounds

Bailey, C. L., Bereman, R. D., Rillema, D. P. & Nowak, R. (1986a). *Inorg. Chem.* **25**, 933–938.

Bailey, C. L., Bereman, R. D., Rillema, D. P. & Nowak, R. (1986b). *Inorg. Chem.* **25**, 3149–3153.

Bernstein, J., Davis, R. E., Shimoni, L. & Chang, N.-L. (1995). *Angew. Chem. Int. Ed. Engl.* **34**, 1555–1573.

Bruker (2005). *CELL_NOW*. Bruker AXS Inc., Madison, Wisconsin, USA.

Bruker (2008). *TWINABS*. Version 2008/2. Bruker AXS Inc., Madison, Wisconsin, USA.

Bruker (2009). *APEX2* (Version 2009.7-0) and *SAINT* (Version 7.66A). Bruker AXS Inc., Madison, Wisconsin, USA.

Bruno, I. J., Cole, J. C., Edgington, P. R., Kessler, M., Macrae, C. F., McCabe, P., Pearson, J. & Taylor, R. (2002). *Acta Cryst.* B**58**, 389–397.

CCDC (2009). *Mercury CSD 2.3* (Build RC4). Cambridge Crystallographic Data Centre, Cambridge, England.

Desiraju, G. R. (2007). *CrystEngComm*, **9**, 91–92.

Domenicano, A., Schultz, G., Hargittai, I., Colapietro, M., Portalone, G., George, P. & Bock, C. W. (1990). *Struct. Chem.* **1**, 107–122.

Gavezzotti, A. (1994). *Acc. Chem. Res.* **27**, 309–314.

Gavezzotti, A. (2008). *Acta Cryst.* B**64**, 401–403.

Gavezzotti, A. & Filippini, G. (1994). *J. Phys. Chem.* **98**, 4831–4837.

Grabowski, S. J. & Krygowski, T. M. (1985). *Acta Cryst.* C**41**, 1224–1226.

Hao, X., Chen, J., Cammers, A., Parkin, S. & Brock, C. P. (2005). *Acta Cryst.* B**61**, 218–226.

Hochgesang, P. J. & Bereman, R. D. (1988). *Inorg. Chim. Acta*, **149**, 69–76.

Kanters, J. A., Kroon, J., Hooft, R., Schouten, A., van Schijndel, J. A. M. & Brandsen, J. (1991). *Croat. Chem. Acta*, **64**, 353–370.

Kumar, M., Papish, E. T. & Zeller, M. (2010). *Acta Cryst.* C**66**, m197–m200.

Macrae, C. F., Bruno, I. J., Chisholm, J. A., Edgington, P. R., McCabe, P., Pidcock, E., Rodriguez-Monge, L., Taylor, R., van de Streek, J. & Wood, P. A. (2008). *J. Appl. Cryst.* **41**, 466–470.

Mandon, D., Giraudon, J.-M., Toupet, L., Sala-Pala, J. & Guerchhais, J. E. (1987). *J. Am. Chem. Soc.* **109**, 3490–3491.

Miry, C., LeBrun, D., Kerbaol, J.-M. & L'Her, M. (2000). *J. Electroanal. Chem.* **494**, 53–59.

Prince, P., Fronczek, F. R. & Gandour, R. D. (1991). *Acta Cryst.* C**47**, 895–898.

Ricciardi, G., Bavoso, A., Ross, A., Leij, F. & Cizov, Y. (1995). *J. Chem. Soc. Dalton Trans.* pp. 2385–2389.

Sheldrick, G. M. (2008). *Acta Cryst.* A**64**, 112–122.

Spek, A. L. (2009). *Acta Cryst.* D**65**, 148–155.

Steed, J. W. (2003). *CrystEngComm*, **5**, 169–179.

Weiss, M. C., Bursten, B., Peng, S. M. & Goedken, V. L. (1976). *J. Am. Chem. Soc.* **98**, 8021–8031.

Weiss, M. C., Gordon, G. & Goedken, V. L. (1977). *Inorg. Chem.* **16**, 305–310.

Westrip, S. P. (2010). *J. Appl. Cryst.* **43**, 920–925.

Wieckowski, T. & Krygowski, T. M. (1985). *Croat. Chem. Acta*, **58**, 5.

Wilson, C. C. & Goeta, A. E. (2004). *Angew. Chem. Int. Ed.* **43**, 2095–2099.

Wooodruff, W. H., Pastor, R. W. & Dabrowiak, J. C. (1976). *J. Am. Chem. Soc.* **98**, 7999–8006.